Am J Cancer Res 2024;14(5):1999-2019
www.ajcr.us /ISSN:2156-6976/ajcr0154163

Original Article

Potential antitumor effects of short-chain fatty acids in breast cancer models

Thaís C Muradás[1], Raquel DS Freitas[1], João IB Gonçalves[1,2], Fernando AC Xavier[1,2], Daniel R Marinowic[1,2]

[1]Programa de Pós-graduação em Medicina e Ciências da Saúde, Escola de Medicina, Pontifícia Universidade Católica do Rio Grande do Sul, Porto Alegre, RS, Brazil; [2]Brain Institute of Rio Grande do Sul, Porto Alegre, RS, Brazil

Received October 30, 2023; Accepted March 13, 2024; Epub May 15, 2024; Published May 30, 2024

Abstract: The effects of short-chain fatty acids (SCFAs) have been explored against cancer due to the crosstalk between gut microbiota alterations and the immune system as a crucial role in cancer development. We evaluated the SCFAs effects in both in vitro and in vivo breast cancer models. In vitro, the SCFAs displayed contrasting effects on viability index, according to the evaluation of breast cancer cells with different phenotypes, human MCF-7, SK-BR-3, MDA-MD-231, or the mouse 4T1 lineage. Acetate displayed minimal effects at concentrations up to 100 mM. Alternatively, propionate increases or reduces cell viability depending on the concentration. Butyrate and valerate showed consistent time- and concentration-dependent effects on the viability of human or mouse breast cancer cells. The selective FFA2 4-CMTB or FFA3 AR420626 receptor agonists failed to overtake the SCFA actions, except by modest inhibitory effects on MDA-MB-231 and 4T1 cell viability. The FFA2 CATPB or FFA3 and β-hydroxybutyrate receptor antagonists lacked significant activity on human cell lines, although CATPB reduced 4T1 cell viability. Butyrate significantly affected cell morphology, clonogenicity, and migration, according to the evaluation of MDA-MB-231 and 4T1 cells. A preliminary examination of in vivo oral effects of butyrate, propionate, or valerate, dosed in prophylactic or therapeutic regimens, on several parameters evaluated in an orthotopic breast cancer model showed a reduction of lung metastasis in post-tumor induction butyrate-treated mice. Overall, the present results indicate that in vitro effects of SCFAs did not rely on FFA2 or FFA3 receptor activation, and they were not mirrored in vivo, at least at the tested conditions. Overall, the present results indicate potential in vitro inhibitory effects of SCFAs in breast cancer, independent of FFA2 or FFA3 receptor activation, and, in the metastatic breast cancer model, the butyrate-dosed therapeutic regimen reduced the number of lung metastases.

Keywords: Short-chain fatty acids, FFA2 and FFA3 receptors, breast cancer, in vitro, in vivo

Introduction

Breast cancer represents the tumor type with the highest worldwide incidence, with an estimated 2.3 million newly detected cases [1]. Besides clinical evaluation, a breast cancer diagnosis is based on immunohistochemistry investigation, considering the positivity for hormone receptors, estrogen (ER+) and progesterone (PR+), the labeling for the human epidermal growth factor receptor 2 (HER2+), and the percentage of Ki67-positive cells (Ki67+), as a marker of cell proliferation index. According to these parameters, breast cancer types are classified into luminal A (ER+ and/or PR+, HER2-, Ki67+ < 20%), luminal B (ER+ and/or PR < 20%, HER2-, Ki67+ ≥ 20%); HER2+ (ER-, PR-, and HER2 overexpressed) or triple-negative breast cancer (TNBC) (ER-, PR-, HER2-) [2]. As for the metastatic TNBC, the recurrence and the relative 5-year survival rates are inferior to other breast cancer subtypes at the metastatic stage, corresponding to 12% and 2.6 years, respectively [3]. Therefore, new therapeutic approaches for managing these scenarios require immediate attention.

Short-chain fatty acids (SCFAs), such as acetate, propionate, and butyrate, are a class of bacterial-derived metabolites that can exert their effects by activating two G protein-coupled receptors, described as FFA2 and FFA3, previously known as GPR43 and GPR41, respectively. They can also modulate alternative cell tar-

https://doi.org/10.62347/ETUQ6763

gets, such as histone deacetylases (HDACs), and immune responses, such as modulation of regulatory T cells (Tregs), activity of dendritic cells and macrophages, production of anti- and pro-inflammatory cytokines, and proliferation of plasma B cell [4, 5]. In breast cancer, SCFAs have been reported as antitumor agents in preclinical studies by affecting several cell mechanisms, such as differentiation, growth arrest, and cell invasion [6-10].

Moreover, depending on their molecular subtypes and histologic index, the FFA2 and FFA3 receptors display highly different expression patterns in human breast tissue samples or cell lines. Clinical studies have postulated that gut microbiota alterations and SCFAs composition may affect breast cancer risk and prognosis [11], suggesting that SCFAs may have a beneficial or adverse influence on breast cancer outcomes depending on the experimental paradigm [12]. Given these critical gaps concerning the role of SCFAs in breast cancer, the present study performed a comprehensive characterization of the effects of SCFAs isolated or compared to selective ligands of FFA2 and FFA3 receptors on different subtypes of breast cancer cells or TNBC metastatic tumors model.

Material and methods

Cell lines and reagents

The human breast cancer cell lines MCF-7 (ER+), SK-BR-3 (HER2+), MDA-MB-231 (TNBC), and the mouse mammary gland cell line 4T1 (TNBC/stage IV breast cancer) were purchased from the Rio de Janeiro Cell Bank (BCRJ, Rio de Janeiro, Brazil). Cells were cultured at 37°C in atmosphere of 5% CO_2 in RPMI-1640 Medium supplemented with 10% fetal bovine serum (FBS), 1% penicillin-streptomycin, and 1% amphotericin B. The common reagents for the cell culture were purchased from Invitrogen™ (Carlsbad, California, USA). Sodium acetate, sodium butyrate, sodium propionate, valeric acid, sodium hydroxybutyrate, 4-Chloro-α-(1-methylethyl)-N-2-thiazolyl-benzene acetamide (4-CMTB), (S)-3-(2-(3-Chlorophenyl) acetamido)-4-(4-(trifluoromethyl)phenyl)butanoic acid (CATPB), and N-(2,5-Dichlorophenyl)-4-(furan-2-yl)-2-methyl-5-oxo-1,4,5,6,7,8-hexahydro-quinoline-3-carboxamide (AR420626) were purchased from Sigma-Aldrich (San Luis, Missouri, EUA).

Cell viability assay

Human and mouse breast cancer cell lines were seeded in triplicate, at a density of 6-8 × 10^3/well, in 96-well plates. Following 24 h for allowing attachment, the cells were incubated with different protocol treatments of each SCFA as described below. Firstly, the effects of the SCFAs, acetate, propionate, butyrate, or valerate incubation, were evaluated. The range of concentrations with log-based increasing concentrations of each SCFA varied from 0.1 to 300 mM, depending on the compound, for 24 h, 48 h, and 96 h. Similarly, the effects of SCFAs were compared with those displayed by the selective FFA2 and FFA3 agonists 4-CMTB (0.3 to 30 μM) and AR420626 (0.1 to 30 μM) or the FFA2 and FFA3 antagonists CATPB (0.1 to 30 μM) and β-hydroxybutyrate (1 to 30 mM), respectively, for 24 h, 48 h, and 96 h. Then, to reproduce the actions of microbiota-derived SCFAs, the effects of a combination of acetate (12 mM), propionate (5 mM) plus butyrate (3 M), or propionate plus valerate (both at 1 mM) after 48 h of incubation were evaluated. All concentrations were chosen either from the previous publications [13-16] or based on screening data of the current study. After treatments, the cell viability was assessed by a 3-(4,5-dimethylthiazol-2yl)-2,5-diphenyl tetrazolium bromide (MTT) assay [17]. The results were analyzed on a spectrophotometer (Spectramax M2, Molecular Devices, CA, USA) at 595 nm and expressed as a percentage of the control from 2-3 independent experiments.

Cell morphology

Three SCFAs, butyrate, propionate, or valerate, were selected at the concentration of 10 mM for the cell morphology analysis from the concentration-response experiments on cell viability. For this purpose, the human MDA-MB-231 or the mouse 4T1 breast cancer cell lineages were plated in triplicate at 2 × 10^5/well in 24-well plates. After allowing 40-50% confluence, the medium was renewed, and the cells were exposed to each SCFA for 48 h. At the end of treatment, the cell morphology was registered using an inverted microscope coupled to a computer (Nikon, ECLIPSE Ts2, Melville, NY, USA). Five fields per well from three independent experiments were captured. The cell perimeter and area were determined as described before [18], with adaptations. The

cell polarity was calculated as the major migration axis length divided by the perpendicular axis length intersecting the nucleus, according to Lamers et al. (2011) [19]. For all measures, data are expressed as the percentage of control.

Cell adhesion

For this protocol, the methodology described by Li et al. (2014) [20] was adopted. Briefly, 96-well plates were coated with 0.1% gelatin overnight. The human MDA-MB-231 or the mouse 4T1 breast cancer cells were treated with butyrate, propionate, or valerate (3, 10, and 30 mM). The FFA2 agonist 4-CMTB (3, 10, and 30 μM) was evaluated in a separate experimental set for comparison purposes. After 48 h of ligand incubation, the cells were seeded (at 2×10^5/well) and incubated for one hour to allow adhesion. The non-adherent cells were removed by PBS washing, and 200 μl of 0.05% MTT solution/well was added. The reaction was stopped by adding 100 μl of DMSO. The results were read on a spectrophotometer (Spectramax M2, Molecular Devices, CA, USA) at 595 nm and expressed as the percentage of control of at least four independent experiments.

Clonogenic assay

The effects of SCFAs on the efficiency of colony formation of the human MDA-MB-231 or the mouse 4T1 breast cancer cells were evaluated. For this purpose, the cells were seeded in 24-well plates in duplicate at a density of 5×10^4 cells/well. After allowing attachment, the cells were incubated with butyrate, propionate, or valerate (3, 10, and 30 mM). After 48 h, the cells were re-plated on a density of 1×10^2 in 6-well plates. Ten days later, the cells were fixed in a 10% formaldehyde solution for 30 minutes and stained with 0.5% crystal violet. The mean number of colonies (as a percentage of control) and the survival fraction were determined from three independent experiments [21].

Cell migration

The ability of SCFAs to alter cell migration was analyzed by the in vitro scratch assay [22] with adaptations. The human MDA-MB-231 or the mouse 4T1 cells were seeded in 24-well plates ($1.25\text{-}2.5 \times 10^5$ cells/well; in triplicate) and allowed to reach 80-90% confluence. Afterward, a wound gap in a cell monolayer was created by scratching a 200-μl pipette tip. After a PBS wash and medium renewal, the cells were treated with butyrate, propionate, or valerate (10 mM). The cell migration was documented at 0, 3, 6, 12, 24, and 48 h, using an inverted microscope coupled to a computer under × 40 magnification (Nikon, ECLIPSE Ts2, Melville, NY, USA). The cell uncovered area from three independent experiments was calculated using NIH Image J 1.52a Software (NIH, Bethesda, MD, USA) and expressed as the percentage of control.

4T1 orthotopic breast cancer spontaneous metastasis mouse model and overall assessments

Female Balb/CJ mice (14-18 g; 2-month old; N = 3-4/group) were obtained from the Center for Experimental Biological Models (PUCRS; CeMBE, Porto Alegre, Rio Grande do Sul, Brazil). The mouse 4T1 breast cancer cells, cultured as previously described, were harvested in 100 μl of PBS and orthotopically injected into the 10^{th} mammary fat pad of the mice [23] formerly anesthetized by a mixture of xylazine (10 mg/kg) and ketamine (100 mg/kg). The tumor-free control group received 100 μl of PBS at the same anatomical site.

Two different protocols of treatment were adopted. In the first protocol, the tumor was induced. The treatment with the SCFAs butyrate (600 mg/kg/day) or propionate (75 mg/kg/day) was given orally from day 14 after tumor inoculation until the day before euthanasia (day 29), completing 15 days of treatment. In the second protocol, the SCFAs butyrate (600 mg/kg/day), propionate (75 mg/kg/day), or valerate (0.3 mg/kg/day) were administered orally for 21 days until tumor induction and followed for more 28 days, ending the day prior euthanasia, completing a 48-day treatment period. In both protocols, control animals received vehicle at the exact schedules of treatment (0.9% NaCl; 10 ml/kg) and the doses of SCFAs were selected from previous data [24-26]. The body weight variation (in g), the tumor volume (in mm^3; tumor length × tumor width × tumor width/2), and the survival rates were recorded at different time points. Mice were maintained in microisolators, equipped with inlet/outlet air filters, under controlled temperature (22 ± 1°C) and humidity (50%-70%), and a light-dark cycle

of 12 h (lights on at 7 AM, lights off at 7 PM). Cages were filled with sterilized wood chip bedding and animals received chow and sterile water *ad libitum*. The general locomotor activity of the animals was measured using an automated open-field system (46 × 46 × 36 cm) equipped with infrared sensors [11]. Following the behavioral analysis, mice were euthanized by 4-5% isoflurane inhalation, and blood and tissue samples were collected. As previously described, the blood was used for hematocrit and neutrophil-lymphocyte ratio (NLR) evaluation [11]. Besides tumor-free carcass and tumor weight assessment, the brain, colon, left femur, kidneys, liver, lungs, and spleen were harvested and weighed (in g). The lungs were also photographed for gross analysis of metastasis. After the tumor and lungs were weighed, the samples were fixed in a 10% formaldehyde solution and submitted to conventional histological processing. Five-µm sections were stained with hematoxylin-eosin. Histological images were captured in a Zeiss AxioImager M2 light microscope (Carl Zeiss, Gottingen, Germany) under ×200 magnification. The procedures followed the current Brazilian guidelines for the care and use of animals for scientific and didactic procedures from the National Council for the Control of Animal Experimentation (CONCEA, Brazil). The local Animal Ethics Committee approved all experimental protocols (PUCRS/CEUA 9011).

Statistical analysis

Data are expressed as mean ± standard error mean (SEM) or median accompanied by the interquartile intervals and maximal and minimum values. Statistical analysis of the in vitro data was performed by one-way (treatment as the outcome) or two-way (treatment and time as variables) analysis of variance (ANOVA), followed by Dunnett's post hoc test, except for the comparison between two groups, when an unpaired Student t-test was used. For the in vivo studies, the statistical analysis was accomplished by one-way (for treatment only) or repeated-measures (treatment effects along the time) ANOVA, followed by Tukey's post hoc test. In some cases, the areas under the curve (AUC) were calculated. The survival rates were analyzed by the Log-rank test for trend. The inhibitory concentration of 50% (IC_{50}) and the corresponding intervals of confidence were calculated using the function [Inhibitor] vs. normalized response. *P* values less than 0.05 were considered indicative of significance. The graphs and statistical analysis were built using the GraphPad Software Prism 9.3.1 for Windows (GraphPad Software; San Diego, California, USA).

Results

SCFAs decrease the cell viability of different breast tumor cell lines

To investigate how different SCFAs affect the viability of breast cancer cells, these were exposed to a range of acetate, propionate, butyrate, or valerate concentrations for 24, 48, and 96 hours.

The treatment with acetate at a concentration of 100 mM significantly decreased the cell viability of MCF-7 cells at 48 h and 96 h (**Figure 1A**). At 100 mM, acetate also significantly reduced the viability of MDA-MB-231 cells at 96 h (**Figure 1C**), but had no evident effect on SK-BR-3 cell viability (**Figure 1B**). The non-physiological concentration of 300 mM significantly decreased cell viability of all tumor cell lines (**Figure 1A-C**), presenting inhibitory rates higher than 90% at 96 h.

Considering propionate, cells were treated at average concentrations ranging from 0.1 to 30 mM. Interestingly, propionate treatment significantly increased cell viability, according to the assessment of MCF-7, SK-BR-3, and MDA-MB-231 cell lines, when tested at 1 mM and 96 h of incubation (**Figure 1D-F**). Conversely, when incubated at 10 and 30 mM, propionate significantly decreased the viability percentages of the three human cell lines at 96 h (**Figure 1D-F**). At this time interval and 30-mM concentration, the maximal inhibition percentages were 58%, 85%, and 48% for MCF-7, SK-BR-3, and MDA-MB-231 cells, respectively. For 24 h and 48 h, there was a significant reduction of MCF-7 viability from 3 to 30 mM (**Figure 1D**).

The SCFA butyrate caused a significant reduction of cell viability at 96 h when tested at 10 and 30 mM, regardless of the evaluated human breast cancer cell lineage, with inhibition percentages around 50% for the higher concentration (**Figure 1G-I**). For the MCF-7 cell line, butyrate also produced significant inhibitory actions at 24 h and 48 h of treatment, at 10 and 30 mM (**Figure 1G**). For the SK-BR-3 and

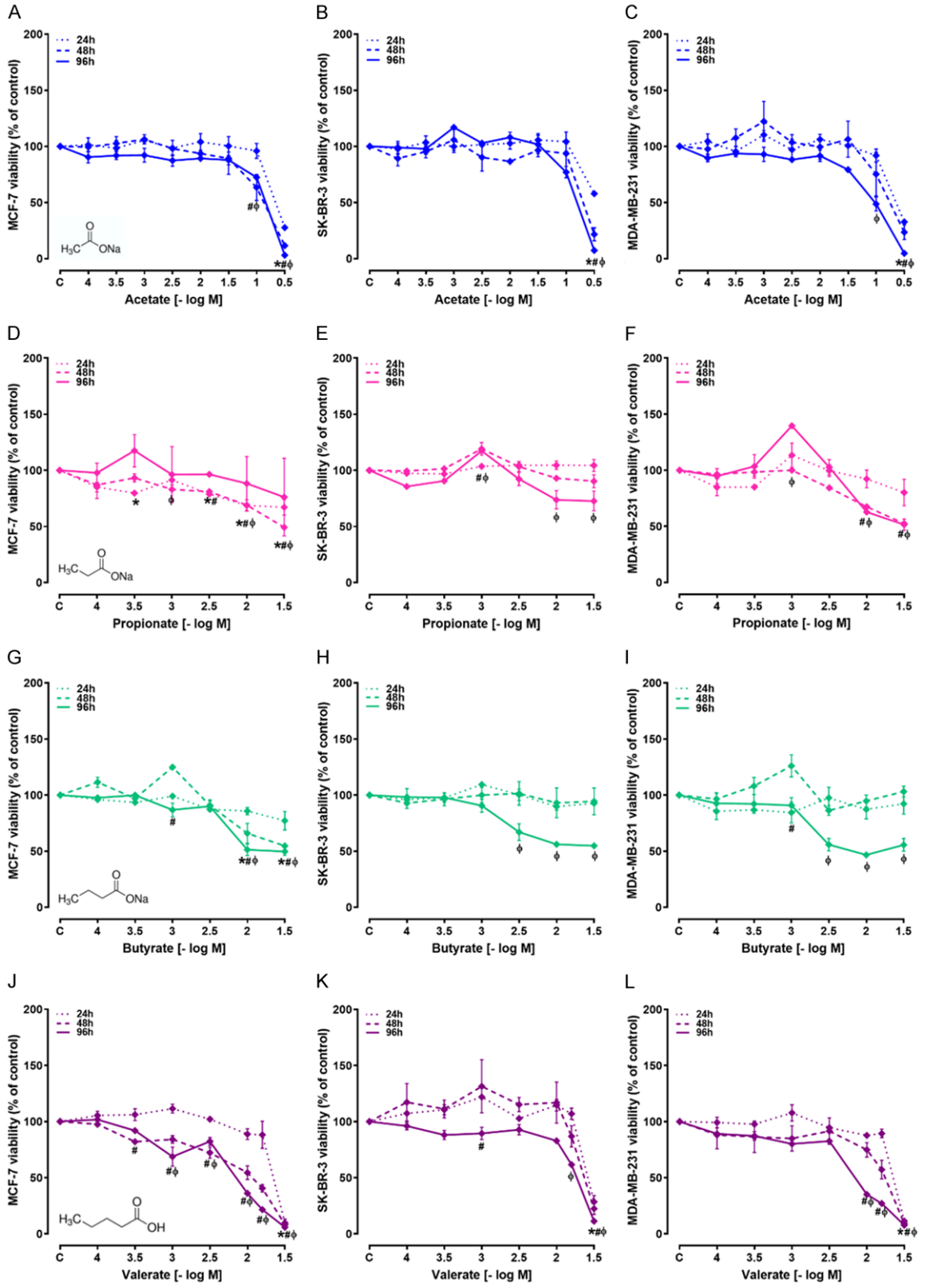

Figure 1. Effects of SCFAs on human breast cancer cell viability. Concentration and time-related effects of acetate (0.1-300 mM; A-C), propionate (0.1-30 mM; D-F), butyrate (0.1-30 mM; G-I) or valerate (0.1-30 mM; J-L) on the viability of MCF-7 (A, D, G, J), SK-BR-3 (B, E, H, K), or MDA-MB-231 (C, F, I, L) human breast cancer cell lineages.

Each point represents the mean of 2-4 independent experiments, and the line indicates the SEM. The results were analyzed by two-way ANOVA followed by Dunnett's post hoc test, considering treatment and time as variables. $^{*,\#,\Phi}P < 0.05$ when comparing the treated vs. control group at 24 h, 48 h, or 96 h incubation, respectively. The chemical structures of each SCFA are provided inside (A, D, G, J).

MDA-MB-231 cells, butyrate displayed significant inhibitory effects at the 3 mM concentration and 96 h of incubation (**Figure 1H** and **1I**).

The exposure of MCF-7, SK-BR-3, and MDA-MB-231 human breast cancer cell lines to valerate produced a significant concentration- and time-dependent blocking of cell viability, with maximal inhibitions > 90%, at 30-mM concentration and 96 h of treatment (**Figure 1J-L**). For this SCFA, the concentration of 15 mM reduced the viability of MCF-7, SK-BR-3, and MDA-MB-231 cells by 78%, 38%, and 73%, respectively. At lower concentrations (0.3 to 10 mM), valerate also significantly inhibited MCF-7 cell viability (**Figure 1J**).

Subsequently, the susceptibility to the inhibitory effects of SCFAs previously observed was tested in the mouse-invasive breast cancer cell line 4T1. The SCFA acetate displayed significant inhibitory effects when tested at the concentrations of 3, 10, and 30 mM, with maximal inhibitions close to 20%, independent of the time-point (**Figure 2A**). Similarly, the treatment with propionate also lessened the viability of the mouse 4T1 cells, at the concentrations of 10 and 30 mM, regardless of the time-point tested (**Figure 2B**). A marked reduction of the mouse 4T1 cell viability was observed after butyrate exposure, at 3, 10, and 30 mM, from 24 h to 96 h of treatment (**Figure 2C**) with maximal inhibition at 30 mM concentration and 48 h of incubation (about 80%). For 48 h, the estimated mean IC_{50} value (in mM; accompanied by the confidence intervals) was 7.3 (ranging from 5.9 to 8.9). Lastly, valerate was able to significantly reduce the viability indexes at 3, 10, and 30 mM, irrespective of the incubation period (**Figure 2D**). As for valerate, the calculated IC_{50} (mM, with confidence intervals) was 9.6 (varying from 6.8 to 13.7), for the time-point of 48 h.

The effects of the combination of the three gut microbiota-derived SCFA acetate (12 mM), propionate (5 mM), and butyrate (3 mM), totaling 20 mM when combined, was evaluated on the viability of human or mouse cell lines, MCF-7 (**Figure 3A**), SK-BR-3 (**Figure 3B**), MDA-MB-231 (**Figure 3C**), or 4T1 (**Figure 3D**). Data showed a trend toward a synergistic action for this combination protocol on mouse 4T1 cell viability but without statistical significance. A combination of valerate plus propionate (both at 1 mM) was also analyzed, but it failed to produce any significant effect in either the human MDA-MB-231 (**Figure 3E**) or the mouse 4T1 (**Figure 3F**) cells.

Overall, our results demonstrate that these SCFAs impact the viability of breast cancer cells, depending on the concentration and duration of exposure.

Selective FFA2 or FFA3 ligands and cell viability

Considering the ability of SCFAs to activate FFA2 and FFA3 receptors, a separate series of experiments were performed to assess the effects of selective ligands for comparison purposes. The selective FFA2 agonist 4-CMTB significantly reduced the viability of the human MDA-MB-231 cell line at concentrations varying from 0.3 to 30 μM, except for 3 μM. For this cell line, the maximal inhibition was observed at 96 h, with a 30-μM concentration (around 20%) (**Figure 4C**). For the SK-BR-3 lineage, 4-CMTB inhibited significantly cell viability at 96 h, without an apparent concentration-related effect (**Figure 4B**). The incubation of 4-CMTB failed to alter the viability of the human MCF-7 (**Figure 4A**) or the mouse 4T1 cell lines (**Figure 2E**). Concerning the FFA2 antagonist CATPB, did not significantly modify the viability of any tested human breast cancer cell lines (**Figure 4D-F**); nevertheless, this antagonist significantly reduced the mouse 4T1 cell viability, in concentrations ranging from 3 to 30 μM (**Figure 2F**). For the latter cell lineage, the percentages of inhibition with CATPB did not exceed 30%, irrespective of the concentration or incubation period.

As for the selective FFA3 agonist AR420626 (0.1 to 30 μM), this compound blocked only MCF-7 cell viability (at 10 μM; 24 h) (**Figure 4G-I**). Alternatively, AR420626 significantly inhibited the viability of mouse 4T1 cells at 3,

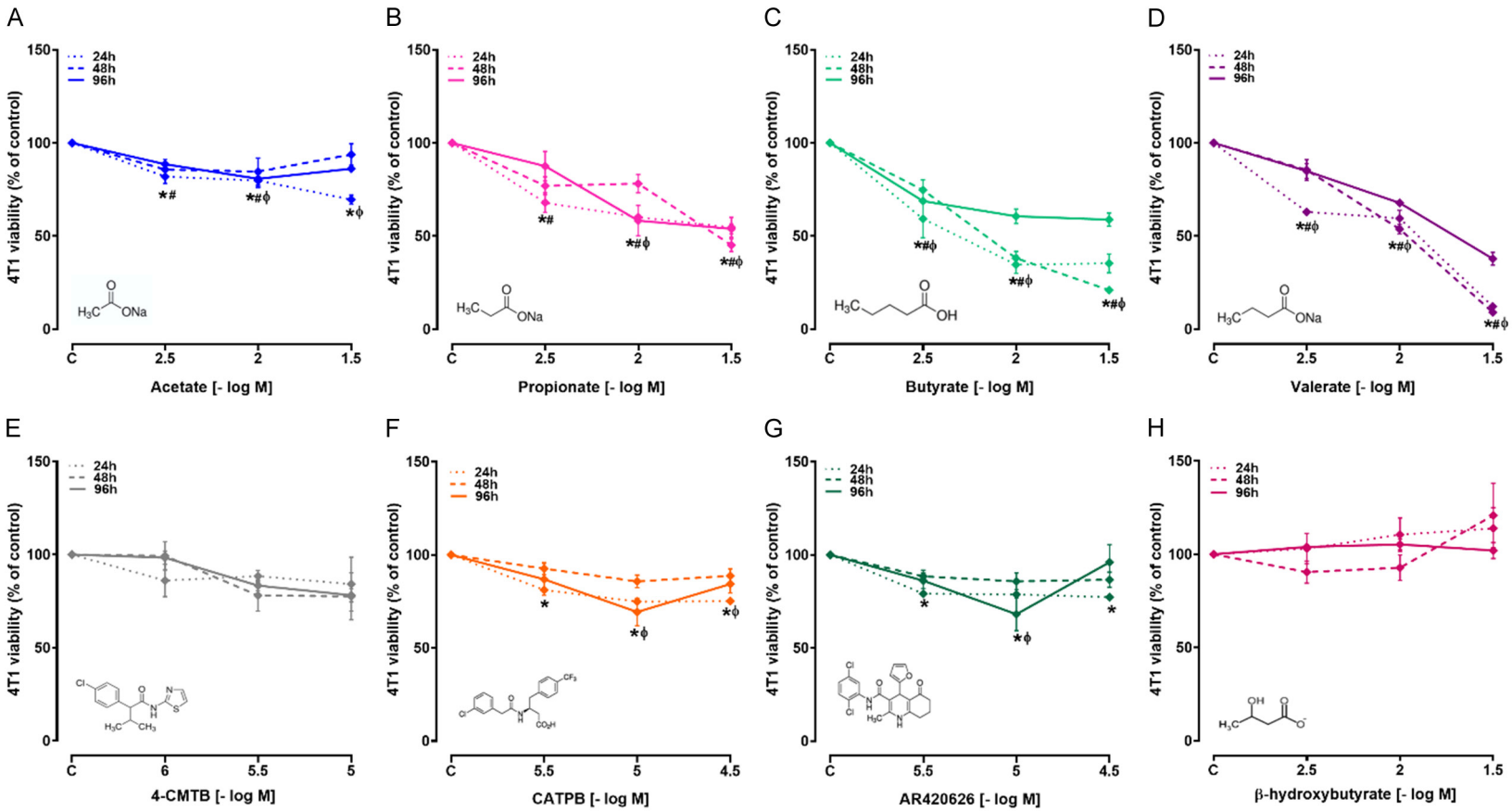

Figure 2. Comparative effects of SCFAs and selective FFA2 and FFA3 ligands on 4T1 cell viability. Concentration and time-related effects of acetate (A), propionate (B), butyrate (C), or valerate (D), all tested at 3-30 mM, on the viability of the mouse mammary gland cell line 4T1. Effects of the selective FFA2 and FFA3 agonists 4-CMTB (1-10 μM; E) and AR420626 (3-30 μM; G), or the FFA2 and FFA3 antagonists CATPB (3-30 μM; F) and β-hydroxybutyrate (3-30 mM; H), respectively, on the viability of the same cell lineage. Each point represents the mean of 2-4 independent experiments, and the line indicates the SEM. The results were analyzed by two-way ANOVA followed by Dunnett's post hoc test, considering treatment and time as variables. $^{*,\#,\Phi}P < 0.05$ when comparing the treated vs. control group at 24 h, 48 h, or 96 h incubation, respectively. The chemical structures of each SCFA are provided inside each corresponding panel.

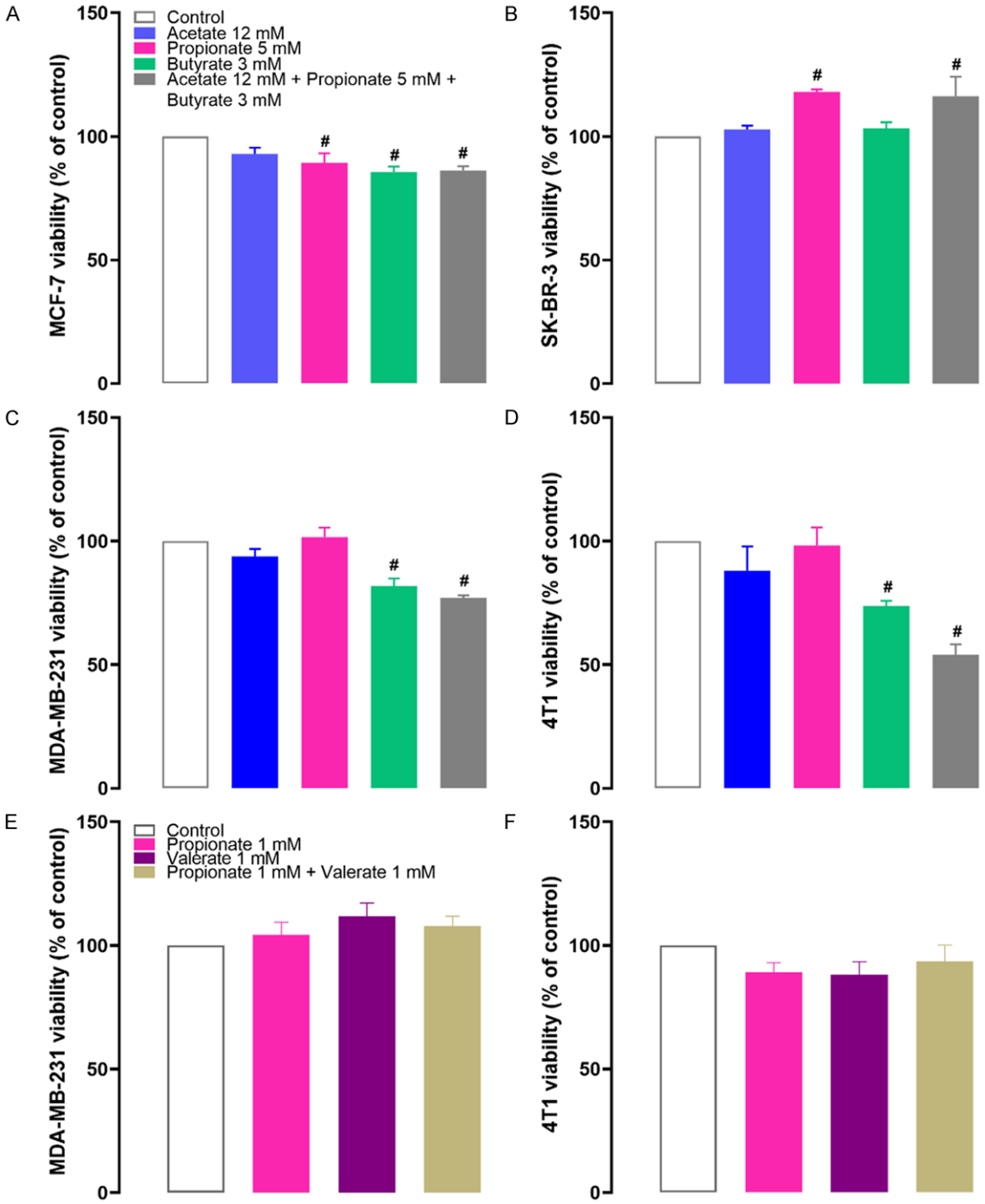

Figure 3. Combination effects of SCFAs on cell viability of breast cancer cells. Effects of acetate (12 mM), propionate (5 mM) plus butyrate (3 M), on the viability of the human MCF-7 (A), SK-BR-3 (B), and MDA-MB-231 (C), or the mouse 4T1 (D) breast cancer cells, after 48 h of incubation. Effects of propionate plus valerate (both at 1 mM) on cell viability of MDA-MB-231 (E), or 4T1 (F) breast cancer cells after 48 h. Each column represents the mean of 3 independent experiments, and the line indicates the SEM. The results were analyzed by one-way ANOVA followed by Tukey's post hoc test. #P < 0.05 when comparing treated vs. control group.

10, and 30 μM, mainly at 24 h of incubation, with a ≈20% reduction (**Figure 2G**). The FFA3 antagonist β-hydroxybutyrate (1 to 30 mM) did not elicit any significant alteration of humans (**Figure 4J-L**) or mice (**Figure 2H**) breast cancer cell viability.

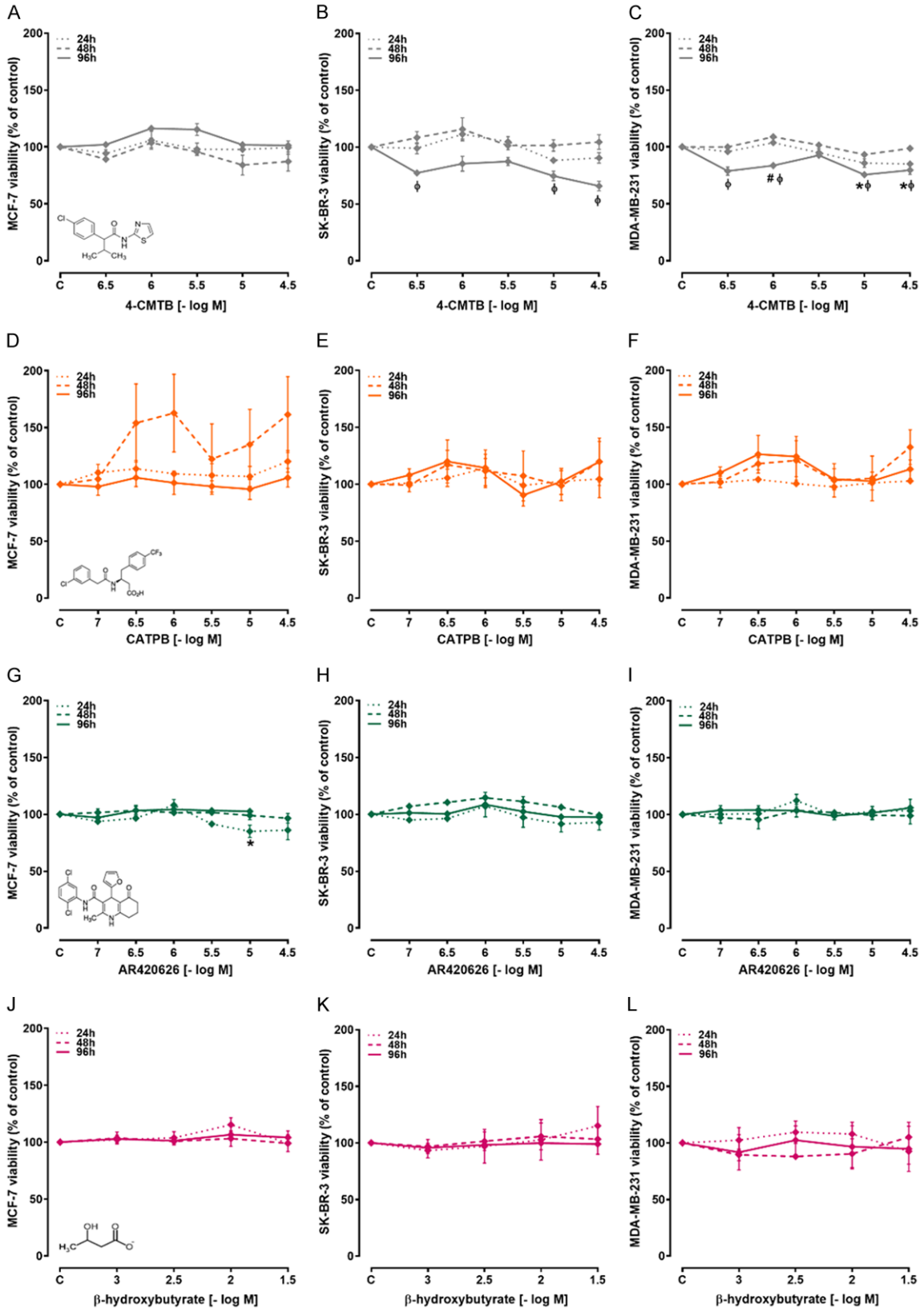

Figure 4. Modulation of selective FFA2 and FFA3 ligands on human breast cancer cell viability. Concentration and time-related effects of the selective FFA2 and FFA3 agonists 4-CMTB (0.3-30 μM; A-C) and AR420626 (0.1-30 μM; G-I), or the FFA2 and FFA3 antagonists CATPB (0.1-30 μM; D-F) and β-hydroxybutyrate (1-30 mM; J-L), respectively,

on the viability of MCF-7 (A, D, G, J), SK-BR-3 (B, E, H, K), or MDA-MB-231 (C, F, I, L) human breast cancer cell lineages. Each point represents the mean of 2-4 independent experiments, and the line indicates the SEM. The results were analyzed by two-way ANOVA followed by Dunnett's post hoc test, considering treatment and time as variables. $^{*,\#,\Phi}P < 0.05$ when comparing the treated vs. control group at 24 h, 48 h, or 96 h incubation, respectively. The chemical structures of the agonists and antagonists are provided inside (A, D, G, J).

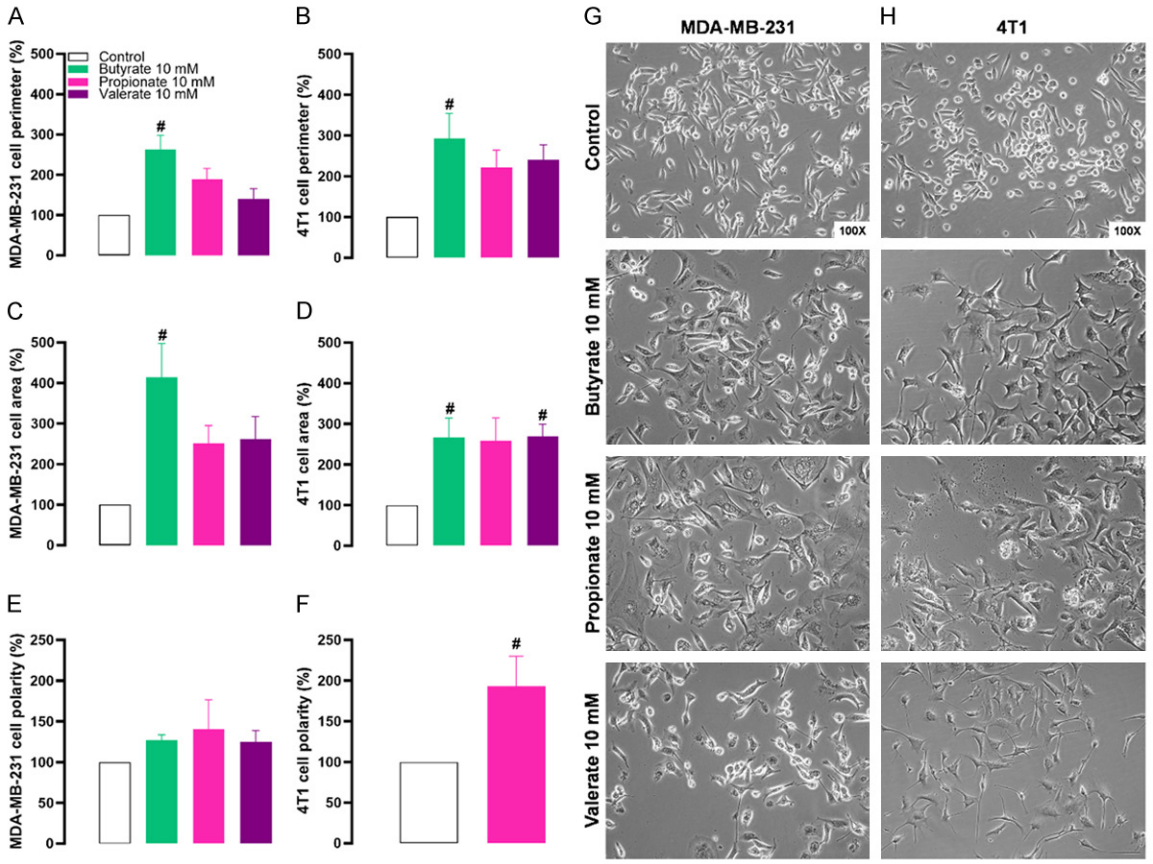

Figure 5. Morphological changes induced by SCFAs in breast cancer cells, MDA-MB-231 and 4T1. Semi-quantitative analysis regarding the morphological changes of the human MDA-MB-231 (A, C, E) or the mouse 4T1 (B, D, F) breast cancer cell lines after exposure to the SCFAs, butyrate, propionate, or valerate, all tested at 10 mM. Data shows the alterations of the perimeter (A, B), the area (C, D), and the cell polarity (E, F). Each column represents the mean of 3 independent experiments, and the line indicates the SEM. The results were analyzed by one-way ANOVA followed by Dunnett's post hoc test, except for (F), for which an unpaired Student t-test was performed. $^{\#}P < 0.05$ when comparing the treated vs. control group at 48 h of incubation. Representative images are showing the morphology of MDA-MB-231 (G) or 4T1 (H) cells in control or treatment groups.

In vitro assessment of breast cancer cell invasiveness

The SCFAs butyrate, propionate, and valerate were selected for the assessment of invasion, adhesion, clonogenicity, and migration assays due to their high efficacy in the previous experiments. Data depicted in **Figure 5** show that butyrate (10 mM) triggered a significant increase in MDA-MB-231 cell perimeter (**Figure 5A**) and area (**Figure 5C**) without modifying the cell polarity index (**Figure 5E**). As for the mouse 4T1 cell lineage, butyrate also led to a significant increase in cell perimeter (**Figure 5B**). The 4T1 cell areas were significantly wider in the butyrate- and valerate-treated groups (both at 10 mM), with a trend toward elevation for propionate treatment (10 mM; $P = 0.06$) (**Figure 5D**). Finally, propionate also induced a significant increase of cell polarity in mouse 4T1 cells (**Figure 5F**). It was not possible to determine the 4T1 cell polarity in butyrate- and valerate-treated groups due to the observed morphological alterations. Repre-

sentative images show the morphology of human MDA-MB-231 (**Figure 5G**) and mouse 4T1 (**Figure 5H**) cells throughout the different experimental groups.

As for cell adhesion, valerate (30 mM) reduced this parameter, according to the evaluation of human MDA-MB-231 cells (**Figure 6A**), whereas this same SCFA (at 3 mM) induced a significant increase in mouse 4T1 cell adhesion (**Figure 6C**). There were no significant alterations of cell adhesion for butyrate or propionate (both tested at 3 to 30 mM), in either MDA-MB-231 or 4T1 cells (**Figure 6A** and **6C**). Considering that 4-CMTB elicited significant effects on MDA-MB-231 cell viability, it was also examined in the cell adhesion assay (3 to 30 μM). However, this FFA2 agonist did not significantly affect the cell adhesion of both cell lines (**Figure 6A** and **6C**). Representative images regarding the cell adhesion assay are provided in **Figure 6B** and **6D** for MDA-MB-231 or 4T1 cells, respectively.

The capacity of forming colonies is a relevant feature of tumor cells. In this evaluation, butyrate significantly inhibited the colony formation of MDA-MB-231 (**Figure 7A**) and 4T1 (**Figure 7D**) cells at 10 and 30 mM concentrations, respectively. The incubation with propionate (3 to 30 mM) significantly diminished the colony numbers of the human MDA-MB-231 (**Figure 7A**) but not the mouse 4T1 (**Figure 7D**) cell line. The incubation with valerate (30 mM) also significantly reduced colony numbers for both tested cell lines (**Figure 7A** and **7D**). The inhibitory actions of SCFAs on clonogenicity were confirmed by the calculation of survival fractions for MDA-MB-231 (**Figure 7B**) and 4T1 (**Figure 7E**) cell lineages. Representative images showing the ability of SCFA to impair the clonogenicity of human MDA-MB-231 or the mouse 4T1 cells are provided in **Figure 7C** and **7F**, correspondingly.

The classical scratching assay was used to verify whether the SCFAs might prevent the migration capability of MDA-MB-231 (**Figure 8A**) and 4T1 (**Figure 8C**) cells. Data showed the cell gap was utterly closed, irrespective of the experimental group at 48 h. For the remaining evaluated time-points (3 to 24 h), there was a mild significant inhibition of cell migration for butyrate (10 mM) regarding the mouse 4T1 cell line. In both cell lineages, no further significant effects were observed for butyrate, propionate, or valerate (all at 10 mM). Representative images for cell migration assay are provided in **Figure 8B** and **8D** for the human MDA-MB-231 and the mouse 4T1 cells, respectively.

In vivo assessment of SCFA effects in a mouse model of metastatic breast cancer

Based on the in vitro findings, we decided to investigate to what extent the SCFAs administration might prevent tumor growth and metastasis. For this, subcutaneous injection of 4T1 cells in female Balb/CJ mice induced an orthotopic model of mammary cancer. In a therapeutic scheme of administration, the effects of oral administration of butyrate (600 mg/kg) and propionate (75 mg/kg), dosed from day 14 to day 29 after tumor injection, were observed (**Figure 9A**). A significant reduction in the number of lung metastasis in butyrate-treated animals (**Figure 9F** and **9G**). However, none of the tested parameters were significantly altered by either butyrate or propionate treatment (**Figure 9B-V**). Considering that the diet and gut microbiota might influence cancer progression on a long-term basis, a preventive protocol of treatment with valerate (0.3 mg/kg), in addition to butyrate (600 mg/kg) and propionate (75 mg/kg), were dosed daily, beginning 21 days before the cell tumor injection, and 28 days following tumor induction, totaling 49 days of treatment (**Figure 10A**). This protocol failed to modify the parameters analyzed (**Figure 10B-Y**).

Discussion

Modifying the immune system through SCFAs and gut microbiota in cancer patients represents a promising strategy in cancer management [5]. Several studies have shown that SCFAs affect cancer progression through different mechanisms [6, 7, 27-29]. However, studies on the impact of SCFAs on breast cancer are superficial, and their role remains unclear. Therefore, this study evaluated the effects of SCFAs on breast cancer cells from different molecular subtypes and in a mouse metastatic breast cancer model.

The SCFAs propionate, butyrate, and valerate demonstrated antitumoral effects in the in vitro screening. On the other hand, the selective FFA2 and FFA3 ligands, besides acetate, dis-

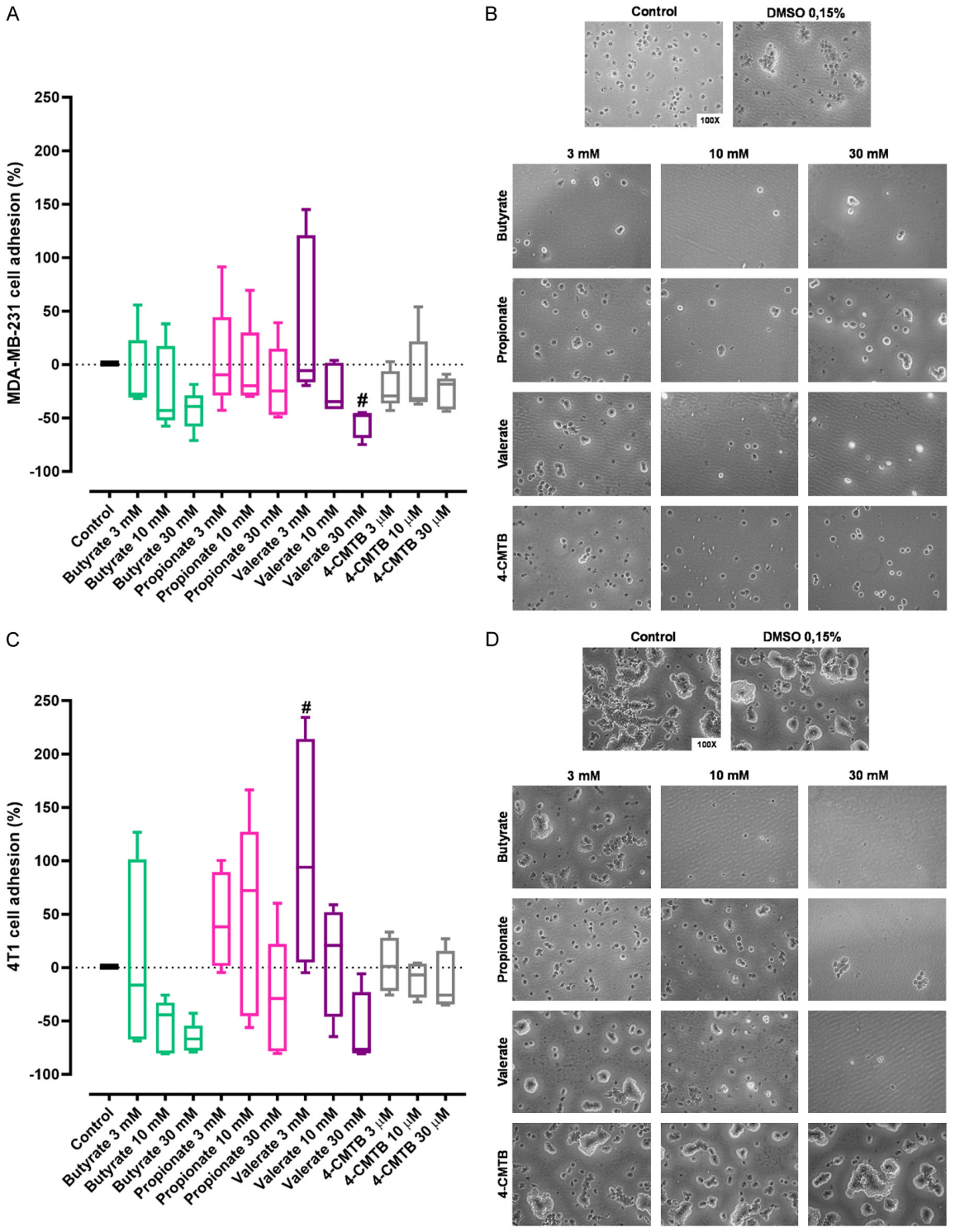

Figure 6. Cell adhesion alterations in response to SCFAs in breast cancer cells, MDA-MB-231 and 4T1. Assessment of adhesion of the human MDA-MB-231 (A) or the mouse 4T1 (C) breast cancer cells after incubation with butyrate (3-30 mM), propionate (3-30 mM), valerate (3-30 mM), or the selective FFA2 agonist 4-CMTB (3-30 µM), for 48 h. The box plots show the median of 4-5 independent experiments with the upper and lower quartiles, whereas the whiskers indicate the maximal and the minimal values. The results were analyzed by one-way ANOVA followed by Dunnett's post hoc test. #P < 0.05 when comparing the treated vs. control group. Representative images are showing the morphology of MDA-MB-231 (B) or 4T1 (D) cells in control or treatment groups.

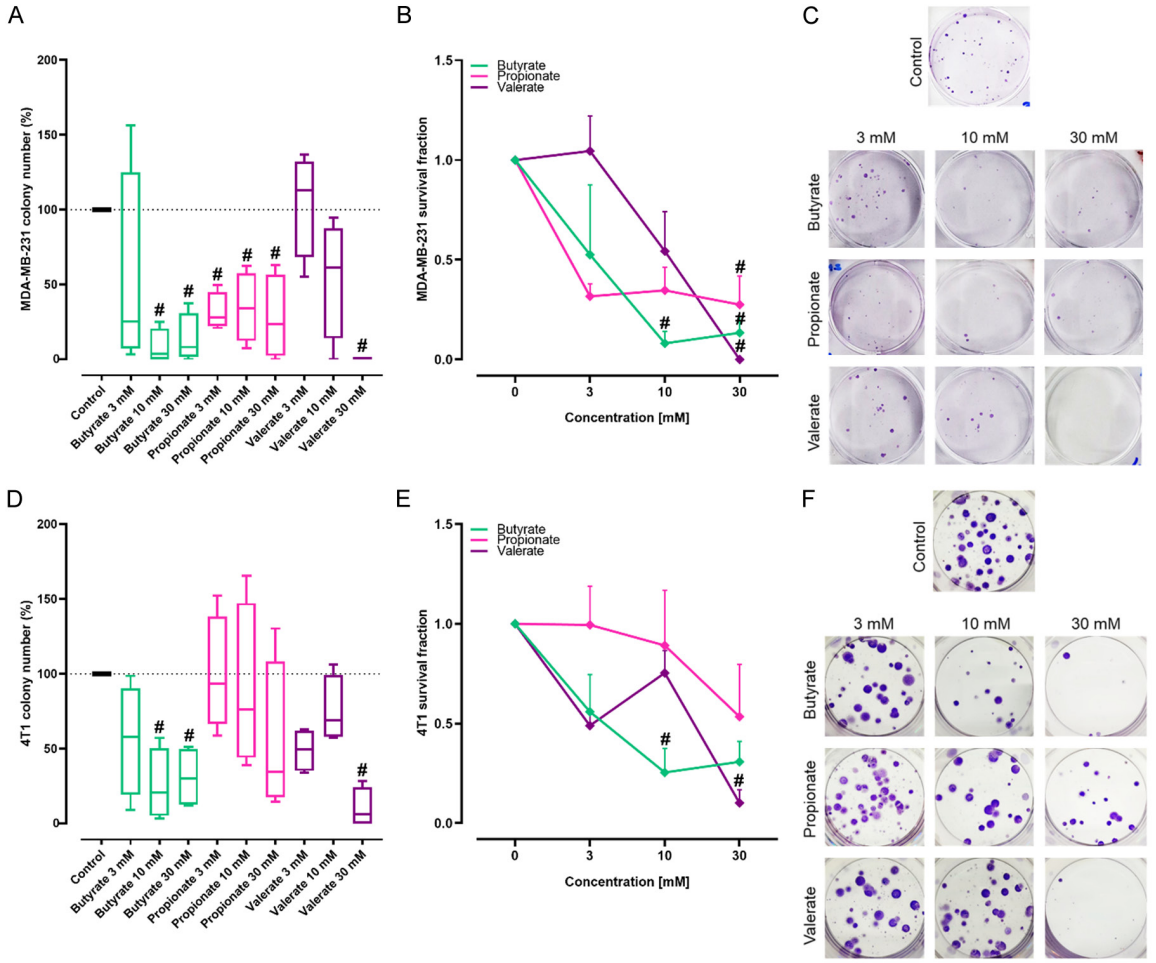

Figure 7. SCFAs reduced the colony formation in breast cancer cells, MDA-MB-231 and 4T1. Examination of colony formation of the human MDA-MB-231 (A, B) or the mouse 4T1 (D, E) breast cancer cells after incubation with butyrate, propionate, or valerate, all tested at 3-30 mM, according to the evaluation of colony numbers (A, D) and survival fraction (B, E). The box plots show the median of 3 independent experiments with the upper and lower quartiles, whereas the whiskers indicate the maximal and the minimal values (A, D). Each point represents the mean of 3 independent experiments, and the line indicates the SEM (B, E). The results were analyzed by one-way ANOVA followed by Dunnett's post hoc test. #P < 0.05 when comparing the treated vs. control group. Representative images are showing the colony formation of MDA-MB-231 (C) or 4T1 (F) cells in control or treatment groups.

played modest outcomes. Initially, cell viability varied after treatment with propionate, butyrate, and valerate according to the cell line, and these discrepancies may be due to mechanisms independent of the FFA2 and FFA3 receptors, such as the HDAC inhibitory capacity of each ligand. Among the SCFAs, butyrate presented the higher efficacy [30, 31]. Our data demonstrated that treatment with acetate promoted an all-or-none pharmacological effect in human breast cancer cell lines and concentration-dependent actions on the 4T1 mouse cell line. In the gastric adenocarcinoma epithelial cell line, high concentrations of acetate induced cytotoxicity and DNA fragmentation and displayed enhanced pro-inflammatory cytokines release [32].

We observed a reduction of cell viability in MDA-MB-231, SK-BR-3, and 4T1 cells when treated with the FFA2 selective synthetic agonist 4-CMTB; this was not observed regarding the MCF-7 cells. Previous data demonstrated that propionate treatment increased CDH1 and reduced cell proliferation through the inhibition of the ERK1/2 pathway in MDA-MB-231 but not in the epithelial-like cells (MCF-7, luminal or BT-474, HER2+) when the FFA2 receptor is overexpressed, when the FFA2 receptor is overexpressed [9]. FFA2 is highly expressed in

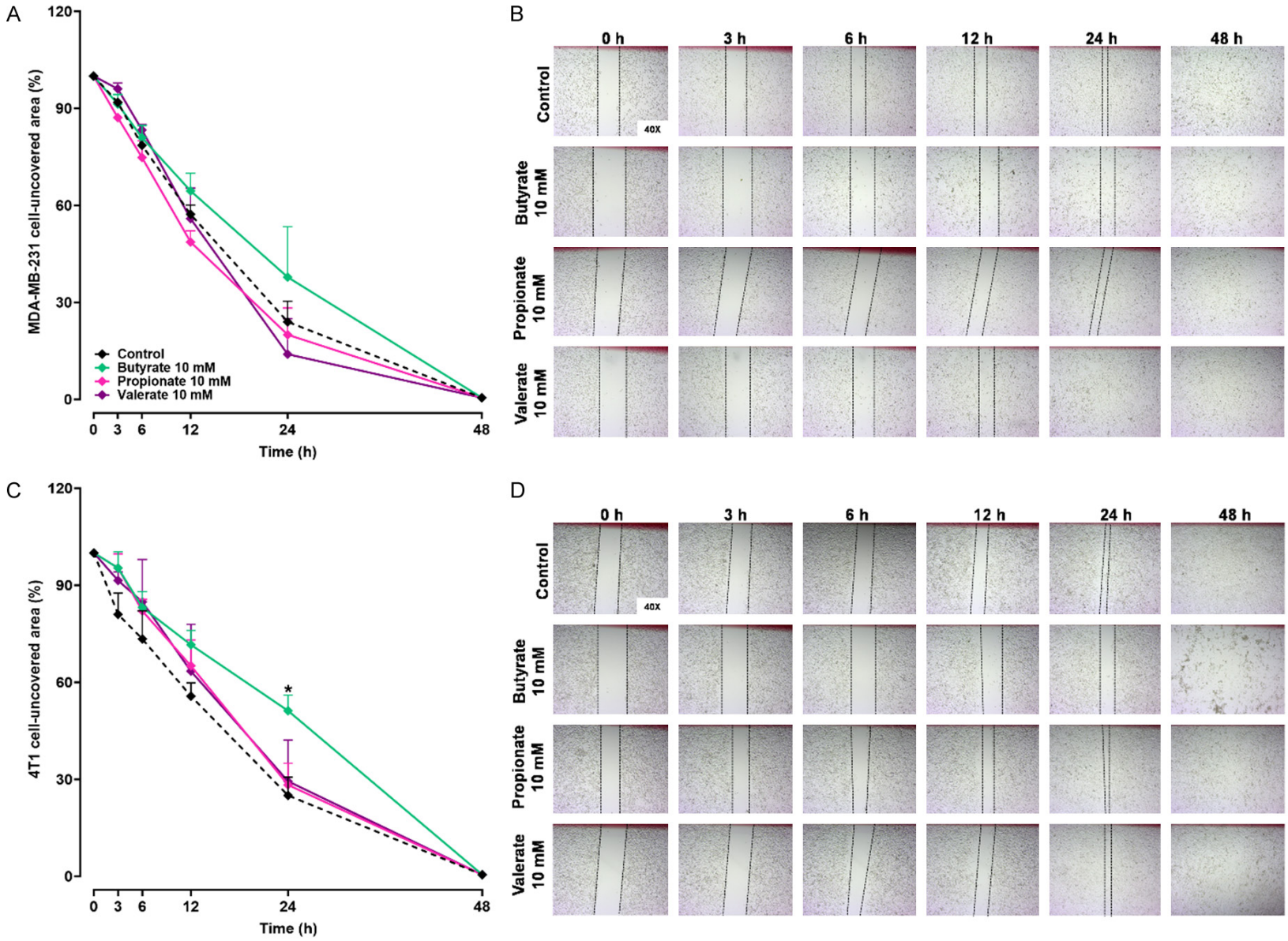

Figure 8. Effects of SCFAs on the migration of breast cancer cells, MDA-MB-231 and 4T1. Time-course for cell migration, measured as the cell-uncovered area, of the human MDA-MB-231 (A) or the mouse 4T1 (C) breast cancer cells after incubation with butyrate, propionate, or valerate, all tested at 10 mM. Each point represents

the mean of 3 independent experiments, and the line indicates the SEM. The results were analyzed by two-way ANOVA followed by Dunnett's post hoc test, considering treatment and time as variables. *P < 0.05 when comparing the treated vs. control group. Representative images are showing the time-related cell migration of MDA-MB-231 (B) or 4T1 (D) cells in control or treatment groups.

breast cancer cell lines compared to FFA3 [7, 10]. Also, the invasive and triple-negative breast carcinoma tissue samples revealed that FFA3 and FFA2 expression are reduced compared to standard breast tissue samples [9]. Interestingly, CATPB and other selective ligands generally did not produce antitumor effects in breast cancer cell lines, indicating that these agonists targeted other mechanisms independent of FFA2 and FFA3 in these cell lines.

Cell morphological changes were observed after propionate, butyrate, and valerate treatments. The MDA-MB-231 cells exhibited a flattened appearance and increased size, suggesting a senescence phenotype, as El Hasasna et al. observed after propionate exposure [33]. Moreover, butyrate and valerate treatments altered the morphology of the MDA-MB-231 and 4T1 cells, developing numerous membrane extensions. This morphology shift could suggest a dendritic process, such as in breast cancer cells exposed to maternal embryonic leucine-zipper kinase (MELK) inhibitor, OTSSP167 [34]. The MELK gene expression is upregulated in breast stem cells and undifferentiated tumors. It is considered an indicator of poor prognosis and treatment resistance, suggesting that the inhibition of this gene might participate in breast cancer control. Similarly, a previous study demonstrated that MCF-7 cells, when exposed to propionate or butyrate, displayed a post-mitotic neuron-like differentiation morphology, indicating a differentiated phenotype and reduced malignant characteristics [6]. These SCFAs induced growth arrest and differentiation of human colon cancer cells associated with histone hyperacetylation [35]. Herein, 4T1 cells displayed these features after propionate treatment; however, only butyrate increased the cell size of MDA-MB-231 and 4T1 cell lines.

The valerate treatment altered cell adhesion in the MDA-MB-231 cell line, and this could be somewhat involved with the dendritic morphology due to the high immunoreactivity for vascular cellular adhesion molecule (VCAM-1) detected in clinically aggressive lymph node sarcoma cells with the same morphology [36]. In addition, the cancer stem cell subpopulation of MDA-MB-231 cells might be transdifferentiated into different phenotypes and morphologies after undergoing cellular damage, modifying its self-renewal capacity to survival mechanism [37]. Notwithstanding, SCFA butyrate has an effect, namely the "butyrate paradox", which portrays the cellular response to be dependent on the level of cellular differentiation to define tumor progression [38].

The effects of treatment with butyrate, propionate, and valerate on the reduction of clonogenic capacity and survival fraction were pronounced in human breast cancer cells. As for the mouse cell line, the capacity to form new colonies and survival fraction were more sensitive to butyrate and valerate only at the highest concentration tested. Likewise, Shi et al. showed that the valerate treatment suppressed the colony formation capacity of human breast cancer cell lines with a regular drug renewal [39]. Butyrate treatment in colon cancer cell lines sensitive to HDAC inhibitors reduced colony formation compared to cell lines resistant to the same inhibitors [40]. Furthermore, in Ewing sarcoma cell lines, the co-treatment of butyrate with zoledronic acid and/or chemotherapeutic agents strongly suppressed the survival fraction and mean size of the colonies [41].

The SCFAs were able to suppress or inhibit cell migration and proliferation. These effects were observed after butyrate treatments in bladder and metastatic colorectal cancer cell lines [27, 28, 42], and the same effects were observed in human breast cancer cell lines after valerate treatment in a concentration- and time-dependent manner mediated by reduced HDAC activity [39]. Interestingly, in 24 h, butyrate incubation significantly inhibited cell migration in the 4T1 cell line, supporting data of the cell viability and colony formation assays after treatment with this same ligand.

Ligands that displayed better antitumoral effects throughout the in vitro screening were selected to be evaluated in a metastatic breast cancer model. Previous studies demonstrated

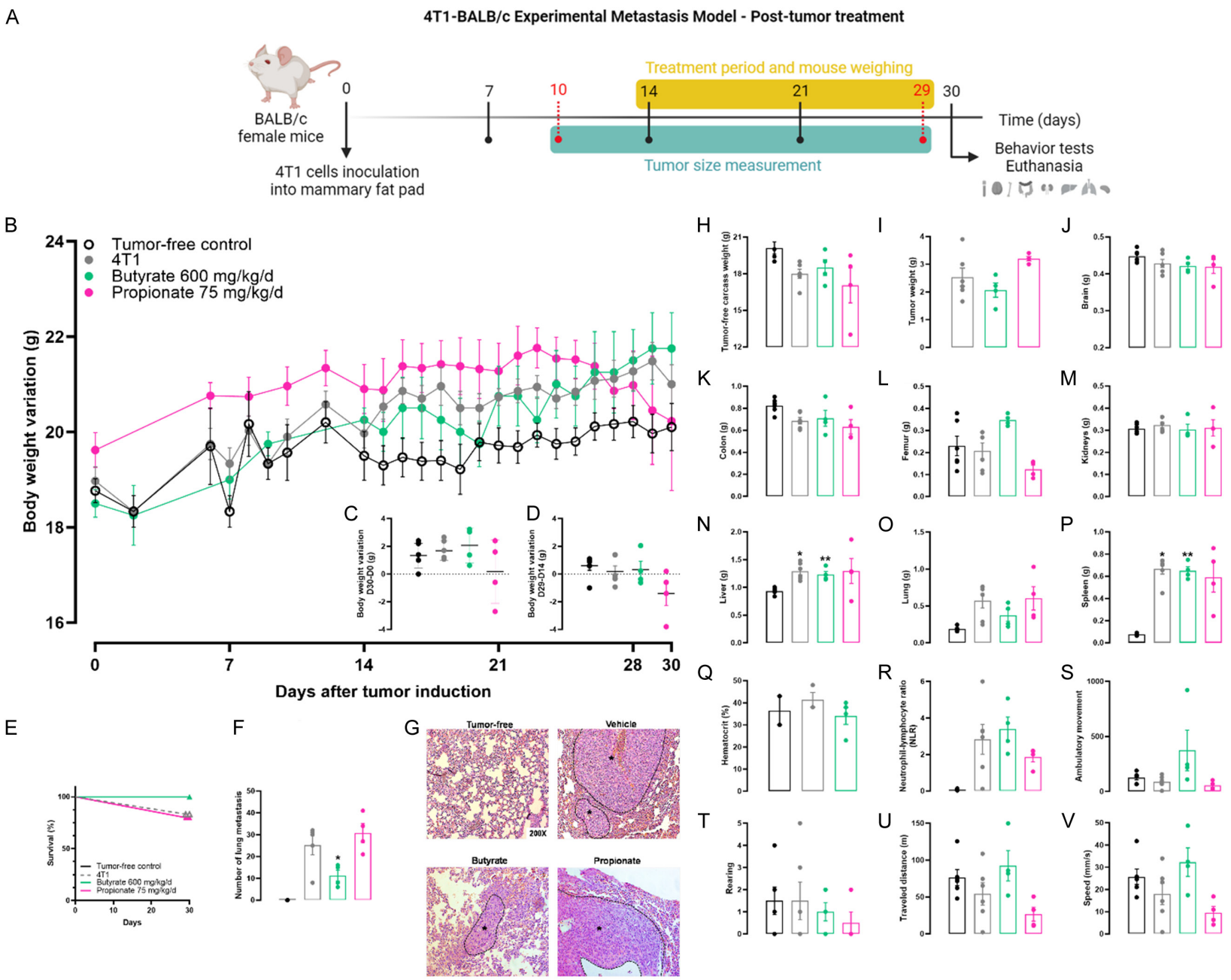
A
4T1-BALB/c Experimental Metastasis Model - Post-tumor treatment
BALB/c female mice
4T1 cells inoculation into mammary fat pad
Treatment period and mouse weighing
Tumor size measurement
Time (days)
Behavior tests
Euthanasia
B
Tumor-free control
4T1
Butyrate 600 mg/kg/d
Propionate 75 mg/kg/d
Body weight variation (g)
Days after tumor induction
C
Body weight variation D30-D0 (g)
D
Body weight variation D29-D14 (g)
E
Survival (%)
Days
F
Number of lung metastasis
G
Tumor-free
Vehicle
Butyrate
Propionate
200X
H
Tumor-free carcass weight (g)
I
Tumor weight (g)
J
Brain (g)
K
Colon (g)
L
Femur (g)
M
Kidneys (g)
N
Liver (g)
O
Lung (g)
P
Spleen (g)
Q
Hematocrit (%)
R
Neutrophil-lymphocyte ratio (NLR)
S
Ambulatory movement
T
Rearing
U
Traveled distance (m)
V
Speed (mm/s)

Figure 9. Reduction of lung metastasis in the butyrate-treated group of therapeutic treatment on metastatic breast cancer model. Oral short-term administration of SCFAs, namely butyrate (600 mg/kg/day), propionate (75 mg/kg/day), or valerate (0.3 mg/kg/day) on the mouse model of metastatic breast cancer induced by 4T1 cell inoculation. (A) Timeline for this experimental protocol: the yellow bar shows the duration of treatment with the SCFA. The tumor was induced on day 0, and the behavioral tasks and euthanasia were performed on day 30. Bodyweight variation (g) of the control and treated groups measured continuously through the entire experimental time (B); as the difference between final (day 30) and initial weight (C); or the difference between days 29 and 14 (D). Evaluation of the different experimental groups regarding the weight of tumor carcass (H), tumor volume (I), brain (J), colon (K), femur (L), kidneys (M), liver (N), lungs (O), spleen (P). Measurement of hematocrit (Q) or neutrophil-to-lymphocyte ratio (NLR) (R). General locomotor activity was measured as ambulatory movement (S), rearing (T), traveled distance (U), and speed (V). A survival curve is depicted in (E). The number of lung metastases is provided in (F). Representative histological images of lung metastasis are shown in (G). Each point or column represents the mean of 4 animals, and the line indicates the SEM. The results were analyzed by one-way ANOVA followed by Tukey's post hoc test, except for the time-course data for which a repeated-measures ANOVA followed by Tukey's multi-comparison test was used. $^{*}P < 0.05$ when comparing treated vs. 4T1 control groups.

that butyrate modulated blood glucose homeostasis and glycogen metabolism in diabetic animals [25], followed by propionate, can be neuroprotective in an epilepsy model [24] and, finally, valerate promoted radioprotection in irradiated mice [26]. Herein, the positive cellular effects produced by these SCFAs were not reproduced by the systemic treatments in the orthotopic breast cancer model. Although daily oral administration of the butyrate therapeutic scheme reduced the number of lung metastases in mice, the sample size was limited, and the results were preliminary. Furthermore, this treatment may have affected metastasis considering a physiological development with fewer cells, unlike primary tumors that expanded faster due to a large amount of necrosis observed in the histological analysis through the intense proliferation of tumor cells without interaction with the host. Regarding other SCFA, recent data demonstrated that the antitumoral effects of propionate in xenographic breast cancer models in mice, by implantation of JIMT-1 or MCF-7 cells, can inhibit tumor growth, by inhibiting STAT3, p38 activation, and stimulating ROS generation [7].

SCFAs have been described as modulators involved in the tumor microenvironment and tumor immunosuppressive therapy [29]. A recent study demonstrated that valerate and butyrate treatments, in safe concentrations, induced high immunostimulatory and antitumor effects of cytotoxic T lymphocytes (CTLs) and chimeric antigen receptor (CAR) T cells in syngeneic murine melanoma and pancreatic cancer models [43]. In this context, high systemic levels of butyrate and propionate in mice and patients affect the antitumor activity of anti-CTLA-4, impairing the expansion of memory T cells and antigen-specific T lymphocytes [8]. These data, added to our study, suggest that the relationship between microbiota-derived SCFAs and immune cells is essential in the involvement of the tumor microenvironment.

Antitumor effects of treatment with cisplatin combined with *Lactobacillus acidophilus* increased survival rate and improved inflammatory profile in the Lewis lung carcinoma mouse model [44]. *Lactobacillus acidophilus* is a probiotic microorganism that produces SCFAs, primarily acetate, propionate, and butyrate, via dietary fiber processing [45, 46]. Recent data suggest that the cumulative effect of butyrate and valerate can increase the capacity of SCFAs to inhibit HDACs, which are known to be a promising and potent target for antitumor therapy [47]. Despite the recommendation for dietary fiber consumption to reduce inflammation and increase breast cancer patients' survival, in addition to butyrate being investigated in clinical trials, alternative strategies for the management of triple-negative tumors and high aggressiveness need to be improved urgently [5].

In summary, this study demonstrated that the natural ligand butyrate showed a significant decrease in malignancy capacity across multiple analyses against MDA-MB-231 and 4T1 cells, and these effects are probably via mechanisms independent of FFA2 or FFA3 receptor activation, including HDAC inhibition. While SCFA did not produce significant beneficial effects in the metastatic breast cancer model, there was a reduction in lung metastases in the therapeutic scheme with butyrate, according to the preliminary findings. It is indicated

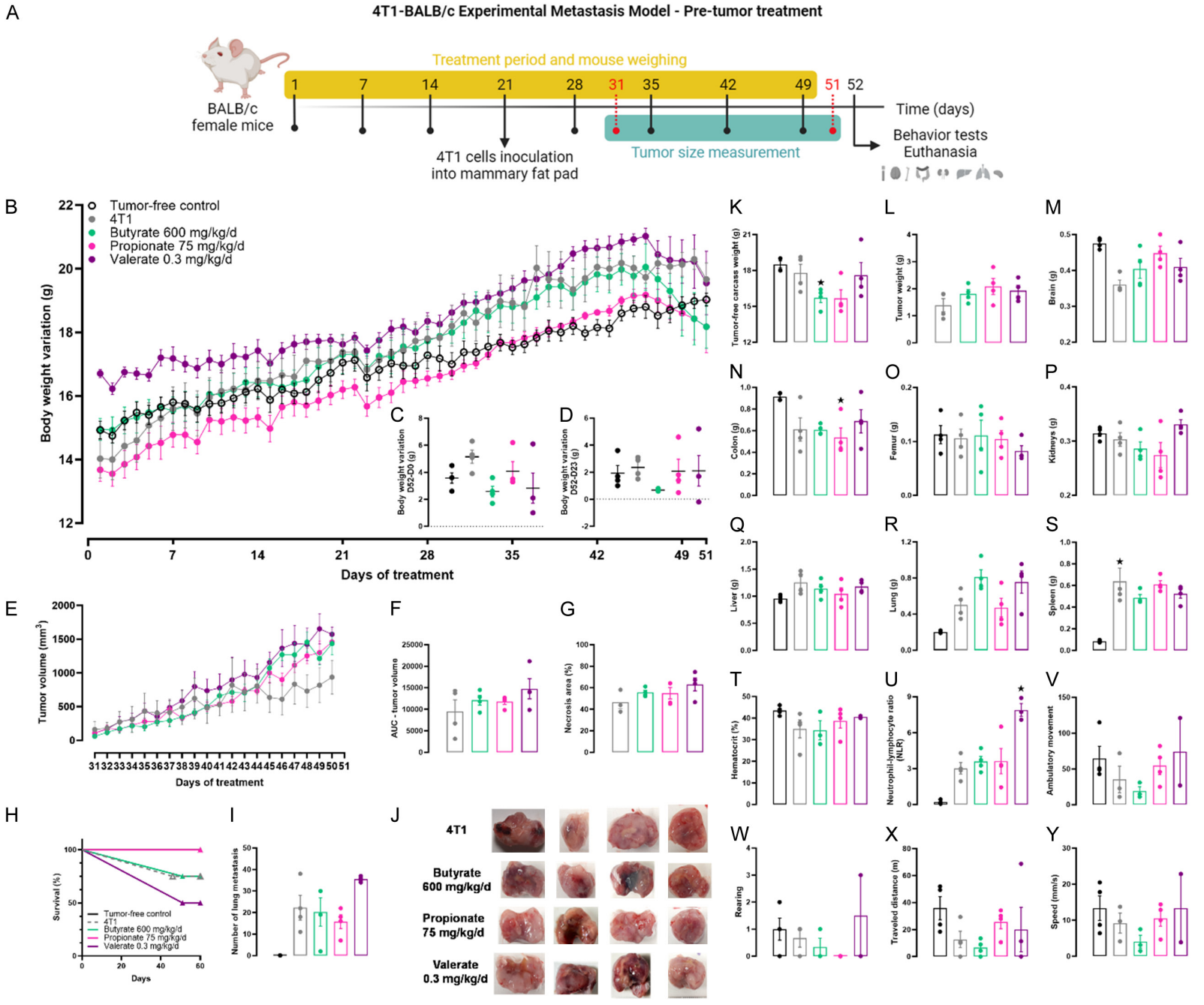
A
4T1-BALB/c Experimental Metastasis Model - Pre-tumor treatment
Treatment period and mouse weighing
BALB/c female mice
1 7 14 21 28 31 35 42 49 51 52
Time (days)
4T1 cells inoculation into mammary fat pad
Tumor size measurement
Behavior tests
Euthanasia
B
Tumor-free control
4T1
Butyrate 600 mg/kg/d
Propionate 75 mg/kg/d
Valerate 0.3 mg/kg/d
Body weight variation (g)
Days of treatment
C
Body weight variation D52-D0 (g)
D
Body weight variation D52-D23 (g)
E
Tumor volume (mm³)
Days of treatment
F
AUC - tumor volume
G
Necrosis area (%)
H
Survival (%)
Days
I
Number of lung metastasis
J
4T1
Butyrate 600 mg/kg/d
Propionate 75 mg/kg/d
Valerate 0.3 mg/kg/d
K
Tumor-free carcass weight (g)
L
Tumor weight (g)
M
Brain (g)
N
Colon (g)
O
Femur (g)
P
Kidneys (g)
Q
Liver (g)
R
Lung (g)
S
Spleen (g)
T
Hematocrit (%)
U
Neutrophil-lymphocyte ratio (NLR)
V
Ambulatory movement
W
Rearing
X
Traveled distance (m)
Y
Speed (mm/s)

Figure 10. Preventive treatment effects of SCFAs on metastatic breast cancer model. Oral long-term administration of SCFAs, butyrate (600 mg/kg/day), propionate (75 mg/kg/day), or valerate (0.3 mg/kg/day) on the mouse model of metastatic breast cancer induced by 4T1 cell inoculation. (A) Timeline for this experimental protocol; the yellow bar shows the duration of treatment with the SCFAs. The tumor was induced at 21 days, and the behavioral tasks were performed on day 51. The tumor volume was measured from day 31 to 51, as indicated by the blue-colored bar. Euthanasia and sample collection were performed on the 52nd experimental day. Bodyweight variation (in g) of the control and treated groups was measured continuously through the entire experimental time (B); as the difference between final (day 52) and initial weight (C); or the difference between days 52 and 23 (D). In vivo tumor volume assessment (in mm^3) (E), accompanied by the area under the curve (AUC; F), and analysis of tumor necrosis areas (G). A survival curve is depicted in (H). The number of lung metastases is provided in (I), accompanied by images regarding the gross evaluation of lung metastasis (J). Appraisal of the different experimental groups regarding the weight of tumor carcass (K), tumor volume (L), brain (M), colon (N), femur (O), kidneys (P), liver (Q), lungs (R), spleen (S). Measurement of hematocrit (T) or neutrophil-to-lymphocyte ratio (NLR) (U). General locomotor activity was measured as ambulatory movement (V), rearing (W), traveled distance (X), and speed (Y). Each point or column represents the mean of 3-4 animals, and the line indicates the SEM. The results were analyzed by one-way ANOVA followed by Tukey's post hoc test, except for the time-course data for which a repeated-measures ANOVA followed by Tukey's multi-comparison test was used. $^{*,\star}P < 0.05$ when comparing treated vs. tumor-free or 4T1 control groups.

that the SCFA butyrate, mainly, might be related to the progression and development of highly invasive breast cancer, and, for this, the discovery of a mechanism that mediates its beneficial effects is necessary to support the development of a promising management strategy for this tumor type.

Acknowledgements

This study was supported by the Coordenação de Aperfeiçoamento de Pessoal de Nível Superior-Brasil (CAPES; Financial Code 001), Conselho Nacional de Desenvolvimento Científico e Tecnológico (CNPq), and Pontifícia Universidade Católica do Rio Grande do Sul (PUCRS). We would like to thank Willian Leitão Pereira for him technical assistance in histological processing. T.C.M., R.D.S.F., J.I.B.G., F.A.C.X., D.R.M., Conselho Nacional de Desenvolvimento Científico e Tecnológico (CNPq) - Financial Code CNPq/MCTI Nº 10/2023 - 408985/2023-2.

Disclosure of conflict of interest

None.

Address correspondence to: Daniel R Marinowic, Programa de Pós-graduação em Medicina e Ciências da Saúde, Escola de Medicina, Pontifícia Universidade Católica do Rio Grande do Sul, Porto Alegre, RS, Brazil. E-mail: daniel.marinowic@pucrs.br

References

[1] Bray F, Ferlay J, Soerjomataram I, Siegel RL, Torre LA and Jemal A. Global cancer statistics 2018: GLOBOCAN estimates of incidence and mortality worldwide for 36 cancers in 185 countries (vol 68, pg 394, 2018). CA Cancer J Clin 2020; 70: 313.

[2] Goldhirsch A, Winer EP, Coates AS, Gelber RD, Piccart-Gebhart M, Thürlimann B and Senn HJ; Panel Members. Personalizing the treatment of women with early breast cancer: highlights of the St Gallen International Expert Consensus on the Primary Therapy of Early Breast Cancer 2013. Ann Oncol 2013; 24: 2206-2223.

[3] Dent R, Trudeau M, Pritchard KI, Hanna WM, Kahn HK, Sawka CA, Lickley LA, Rawlinson E, Sun P and Narod SA. Triple-negative breast cancer: Clinical features and patterns of recurrence. Clin Cancer Res 2007; 13: 4429-4434.

[4] Milligan G, ShimpukadE B, Ulven T and Hudson BD. Complex pharmacology of free fatty acid receptors. Chem Rev 2017; 117: 67-110.

[5] Mirzaei R, Afaghi A, Babakhani S, Sohrabi MR, Hosseini-Fard SR, Babolhavaeji K, Khani Ali Akbari S, Yousefimashouf R and Karampoor S. Role of microbiota-derived short-chain fatty acids in cancer development and prevention. Biomed Pharmacother 2021; 139: 111619.

[6] Semaan J, El-Hakim S, Ibrahim JN, Safi R, Elnar AA and El Boustany C. Comparative effect of sodium butyrate and sodium propionate on proliferation, cell cycle and apoptosis in human breast cancer cells MCF-7. Breast Cancer 2020; 27: 696-705.

[7] Park HS, Han JH, Park JW, Lee DH, Jang KW, Lee M, Heo KS and Myung CS. Sodium propionate exerts anticancer effect in mice bearing breast cancer cell xenograft by regulating JAK2/STAT3/ROS/p38 MAPK signaling. Acta Pharmacol Sin 2021; 42: 1311-1323.

[8] Coutzac C, Jouniaux JM, Paci A, Schmidt J, Mallardo D, Seck A, Asvatourian V, Cassard L, Saulnier P, Lacroix L, Woerther PL, Vozy A, Naigeon M, Nebot-Bral L, Desbois M, Simeone E, Mateus C, Boselli L, Grivel J, Soularue E, Lep-

age P, Carbonnel F, Ascierto PA, Robert C and Chaput N. Systemic short chain fatty acids limit antitumor effect of CTLA-4 blockade in hosts with cancer. Nat Commun 2020; 11: 2168.
[9] Thirunavukkarasan M, Wang C, Rao A, Hind T, Teo YR, Siddiquee AA, Goghari MAI, Kumar AP and Herr DR. Short-chain fatty acid receptors inhibit invasive phenotypes in breast cancer cells. PLoS One 2017; 12: e0186334.
[10] Yonezawa T, Kobayashi Y and Obara Y. Short-chain fatty acids induce acute phosphorylation of the p38 mitogen-activated protein kinase/heat shock protein 27 pathway via GPR43 in the MCF-7 human breast cancer cell line. Cell Signal 2007; 19: 185-193.
[11] Freitas RDS, Muradás TC, Dagnino APA, Rost FL, Costa KM, Venturin GT, Greggio S, da Costa JC and Campos MM. Targeting FFA1 and FFA4 receptors in cancer-induced cachexia. Am J Physiol Endocrinol Metab 2020; 319: E877-E892.
[12] Miko E, Kovacs T, Sebo E, Toth J, Csonka T, Ujlaki G, Sipos A, Szabo J, Mehes G and Bai P. Microbiome-microbial metabolome-cancer cell interactions in breast cancer-familiar, but unexplored. Cells 2019; 8: 293.
[13] Shukla SK, Gebregiworgis T, Purohit V, Chaika NV, Gunda V, Radhakrishnan P, Mehla K, Pipinos II, Powers R, Yu F and Singh PK. Metabolic reprogramming induced by ketone bodies diminishes pancreatic cancer cachexia. Cancer Metab 2014; 2: 18.
[14] Lorza-Gil E, Kaiser G, Rexen Ulven E, König GM, Gerst F, Oquendo MB, Birkenfeld AL, Häring HU, Kostenis E, Ulven T and Ullrich S. FFA2-, but not FFA3-agonists inhibit GSIS of human pseudoislets: a comparative study with mouse islets and rat INS-1E cells. Sci Rep 2020; 10: 16497.
[15] Mikami D, Kobayashi M, Uwada J, Yazawa T, Kamiyama K, Nishimori K, Nishikawa Y, Nishikawa S, Yokoi S, Taniguchi T and Iwano M. AR420626, a selective agonist of GPR41/FFA3, suppresses growth of hepatocellular carcinoma cells by inducing apoptosis via HDAC inhibition. Ther Adv Med Oncol 2020; 12: 1758835920913432.
[16] Zhan K, Gong X, Chen Y, Jiang M, Yang T and Zhao G. Short-chain fatty acids regulate the immune responses via G protein-coupled receptor 41 in bovine rumen epithelial cells. Front Immunol 2019; 10: 2042.
[17] Mosmann T. Rapid colorimetric assay for cellular growth and survival: application to proliferation and cytotoxicity assays. J Immunol Methods 1983; 65: 55-63.
[18] Radaic A, Joo NE, Jeong SH, Yoo SI, Kotov N and Kapila YL. Phosphatidylserine-gold nanoparticles (PS-AuNP) induce prostate and breast cancer cell apoptosis. Pharmaceutics 2021; 13: 1094.
[19] Lamers ML, Almeida ME, Vicente-Manzanares M, Horwitz AF and Santos MF. High glucose-mediated oxidative stress impairs cell migration. PLoS One 2011; 6: e22865.
[20] Li J, Qiu DM, Chen SH, Cao SP and Xia XL. Suppression of human breast cancer cell metastasis by coptisine in vitro. Asian Pac J Cancer Prev 2014; 15: 5747-5751.
[21] Franken NA, Rodermond HM, Stap J, Haveman J and van Bree C. Clonogenic assay of cells in vitro. Nat Protoc 2006; 1: 2315-2319.
[22] Liang CC, Park AY and Guan JL. In vitro scratch assay: a convenient and inexpensive method for analysis of cell migration in vitro. Nat Protoc 2007; 2: 329-333.
[23] Khadge S, Thiele GM, Sharp JG, McGuire TR, Klassen LW, Black PN, DiRusso CC, Cook L and Talmadge JE. Long-chain omega-3 polyunsaturated fatty acids decrease mammary tumor growth, multiorgan metastasis and enhance survival. Clin Exp Metastasis 2018; 35: 797-818.
[24] Cheng Y, Mai Q, Zeng X, Wang H, Xiao Y, Tang L, Li J, Zhang Y and Ding H. Propionate relieves pentylenetetrazol-induced seizures, consequent mitochondrial disruption, neuron necrosis and neurological deficits in mice. Biochem Pharmacol 2019; 169: 113607.
[25] Zhang WQ, Zhao TT, Gui DK, Gao CL, Gu JL, Gan WJ, Huang W, Xu Y, Zhou H, Chen WN, Liu ZL and Xu YH. Sodium butyrate improves liver glycogen metabolism in type 2 diabetes mellitus. J Agric Food Chem 2019; 67: 7694-7705.
[26] Li Y, Dong J, Xiao H, Zhang S, Wang B, Cui M and Fan S. Gut commensal derived-valeric acid protects against radiation injuries. Gut Microbes 2020; 11: 789-806.
[27] Wang F, Wu H, Fan M, Yu R, Zhang Y, Liu J, Zhou X, Cai Y, Huang S, Hu Z and Jin X. Sodium butyrate inhibits migration and induces AMPK-mTOR pathway-dependent autophagy and ROS-mediated apoptosis via the miR-139-5p/Bmi-1 axis in human bladder cancer cells. FASEB J 2020; 34: 4266-4282.
[28] Wang W, Fang D, Zhang H, Xue J, Wangchuk D, Du J and Jiang L. Sodium butyrate selectively kills cancer cells and inhibits migration in colorectal cancer by targeting thioredoxin-1. Onco Targets Ther 2020; 13: 4691-4704.
[29] Qiu Q, Lin Y, Ma Y, Li X, Liang J, Chen Z, Liu K, Huang Y, Luo H, Huang R and Luo L. Exploring the emerging role of the gut microbiota and tumor microenvironment in cancer immunotherapy. Front Immunol 2021; 11: 612202.
[30] Cousens LS, Gallwitz D and Alberts BM. Different accessibilities in chromatin to histone acetylase. J Biol Chem 1979; 254: 1716-1723.

[31] Sunkara LT, Jiang W and Zhang G. Modulation of antimicrobial host defense peptide gene expression by free fatty acids. PLoS One 2012; 7: e49558.
[32] Xia Y, Zhang XL, Jin F, Wang QX, Xiao R, Hao ZH, Gui QD and Sun J. Apoptotic effect of sodium acetate on a human gastric adenocarcinoma epithelial cell line. Genet Mol Res 2016; 15.
[33] El Hasasna H, Athamneh K, Al Samri H, Karuvantevida N, Al Dhaheri Y, Hisaindee S, Ramadan G, Al Tamimi N, AbuQamar S, Eid A and Iratni R. Rhus coriaria induces senescence and autophagic cell death in breast cancer cells through a mechanism involving p38 and ERK1/2 activation. Sci Rep 2015; 5: 13013.
[34] Simon M, Mesmar F, Helguero L and Williams C. Genome-wide effects of MELK-inhibitor in triple-negative breast cancer cells indicate context-dependent response with p53 as a key determinant. PLoS One 2017; 12: e0172832.
[35] Hinnebusch BF, Meng S, Wu JT, Archer SY and Hodin RA. The effects of short-chain fatty acids on human colon cancer cell phenotype are associated with histone hyperacetylation. J Nutr 2002; 132: 1012-1017.
[36] Jones D, Amin M, Ordonez NG, Glassman AB, Hayes KJ and Medeiros LJ. Reticulum cell sarcoma of lymph node with mixed dendritic and fibroblastic features. Mod Pathol 2001; 14: 1059-1067.
[37] Liu TJ, Sun BC, Zhao XL, Zhao XM, Sun T, Gu Q, Yao Z, Dong XY, Zhao N and Liu N. CD133+ cells with cancer stem cell characteristics associates with vasculogenic mimicry in triple-negative breast cancer. Oncogene 2013; 32: 544-553.
[38] Ryu SH, Kaiko GE and Stappenbeck TS. Cellular differentiation: potential insight into butyrate paradox? Mol Cell Oncol 2018; 5: e1212685.
[39] Shi F, Li Y, Han R, Fu A, Wang R, Nusbaum O, Qin Q, Chen X, Hou L and Zhu Y. Valerian and valeric acid inhibit growth of breast cancer cells possibly by mediating epigenetic modifications. Sci Rep 2021; 11: 2519.
[40] Wilson AJ, Chueh AC, Tögel L, Corner GA, Ahmed N, Goel S, Byun DS, Nasser S, Houston MA, Jhawer M, Smartt HJ, Murray LB, Nicholas C, Heerdt BG, Arango D, Augenlicht LH and Mariadason JM. Apoptotic sensitivity of colon cancer cells to histone deacetylase inhibitors is mediated by an Sp1/Sp3-activated transcriptional program involving immediate-early gene induction. Cancer Res 2010; 70: 609-620.
[41] Dos Santos MP, De Farias CB, Roesler R, Brunetto AL and Abujamra AL. In vitro antitumor effect of sodium butyrate and zoledronic acid combined with traditional chemotherapeutic drugs: a paradigm of synergistic molecular targeting in the treatment of Ewing sarcoma. Oncol Rep 2014; 31: 955-968.
[42] Li Q, Ding C, Meng T, Lu W, Liu W, Hao H and Cao L. Butyrate suppresses motility of colorectal cancer cells via deactivating Akt/ERK signaling in histone deacetylase dependent manner. J Pharmacol Sci 2017; 135: 148-155.
[43] Luu M, Riester Z, Baldrich A, Reichardt N, Yuille S, Busetti A, Klein M, Wempe A, Leister H, Raifer H, Picard F, Muhammad K, Ohl K, Romero R, Fischer F, Bauer CA, Huber M, Gress TM, Lauth M, Danhof S, Bopp T, Nerreter T, Mulder IE, Steinhoff U, Hudecek M and Visekruna A. Microbial short-chain fatty acids modulate CD8(+) T cell responses and improve adoptive immunotherapy for cancer. Nat Commun 2021; 12: 4077.
[44] Gui QF, Lu HF, Zhang CX, Xu ZR and Yang YM. Well-balanced commensal microbiota contributes to anti-cancer response in a lung cancer mouse model. Genet Mol Res 2015; 14: 5642-5651.
[45] Andrews MG, Subramanian L and Kriegstein AR. mTOR signaling regulates the morphology and migration of outer radial glia in developing human cortex. Elife 2020; 9: e58737.
[46] Markowiak-Kopeć P and Śliżewska K. The effect of probiotics on the production of short-chain fatty acids by human intestinal microbiome. Nutrients 2020; 12: 1107.
[47] Yuille S, Reichardt N, Panda S, Dunbar H and Mulder IE. Human gut bacteria as potent class I histone deacetylase inhibitors in vitro through production of butyric acid and valeric acid. PLoS One 2018; 13: e0201073.